AD-A176 054 CHARGE DENSITY WAVES IN THE MIXED-VALENCE TWO-DIMENSIONAL METAL K3CU8S6(U) NORTH CAROLINA UNIV AT CHAPEL HILL DEPT OF CHEMISTRY L W HAAR ET AL. 1/1

UNCLASSIFIED 07 JAN 87 TR-25 N00014-76-C-0016 F/G 11/6 NL

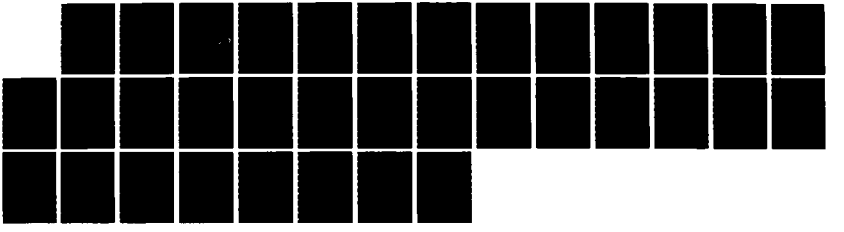

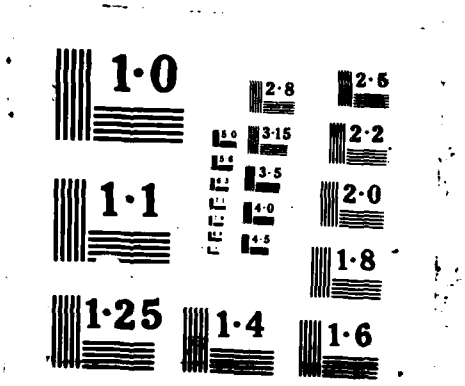
1·0
1·1
1·25
1·4
1·6
1·8
2·0
2·2
2·5
2·8
3·15
3·5
4·0
4·5

UI
SECU

AD-A176 054

ORT DOCUMENTATION PAGE

1a. REPORT SECURITY CLASSIFICATION: Unclassified	1b. RESTRICTIVE MARKINGS
2a. SECURITY CLASSIFICATION AUTHORITY	3. DISTRIBUTION/AVAILABILITY OF REPORT: Approved for Public Release Distribution Unlimited
2b. DECLASSIFICATION/DOWNGRADING SCHEDULE	
4. PERFORMING ORGANIZATION REPORT NUMBER(S)	5. MONITORING ORGANIZATION REPORT NUMBER(S)
6a. NAME OF PERFORMING ORGANIZATION: Department of Chemistry, University of North Carolina; 6b. OFFICE SYMBOL (If applicable)	7a. NAME OF MONITORING ORGANIZATION: Office of Naval Research
6c. ADDRESS (City, State, and ZIP Code): Chapel Hill, North Carolina 27514	7b. ADDRESS (City, State, and ZIP Code): Department of the Navy, Arlington, VA 22217
8a. NAME OF FUNDING/SPONSORING ORGANIZATION; 8b. OFFICE SYMBOL (If applicable)	9. PROCUREMENT INSTRUMENT IDENTIFICATION NUMBER: N00014-76-C-0816
8c. ADDRESS (City, State, and ZIP Code)	10. SOURCE OF FUNDING NUMBERS: PROGRAM ELEMENT NO.; PROJECT NO.; TASK NO: NR 053-617; WORK UNIT ACCESSION NO

11. TITLE (Include Security Classification)
Unclassified: Charge Density Waves in the Mixed-Valence Two-Dimensional Metal, $K_3Cu_8S_6$

12. PERSONAL AUTHOR(S) ter Haar, L. W.; Di Salvo, F. J.; Bair, H. E.; Fleming, R. M.; Waszczak, J. V.; Hatfield, W. E.

13a. TYPE OF REPORT	13b. TIME COVERED	14. DATE OF REPORT (Year, Month, Day)	15. PAGE COUNT
Technical Report	FROM _____ TO _____	1987, Jan 7	32

16. SUPPLEMENTARY NOTATION

17. COSATI CODES		
FIELD	GROUP	SUB-GROUP

18. SUBJECT TERMS (Continue on reverse if necessary and identify by block number)
transition metal compounds electrical conductivities magnetic susceptibility charge density waves mixed valence compounds chain compounds

19. ABSTRACT (Continue on reverse if necessary and identify by block number)

The synthetic conditions for the preparation of KCu_4S_3, $K_3Cu_8S_6$, and KCu_3S_2 have been carefully defined. $K_3Cu_8S_6$ is apparently a kinetic phase and must be trapped with a minimum amount of either KCu_4S_3 or KCu_3S_2. Magnetic susceptibility and electrical resistivity data display behavior typical of CDW systems. In view of the low-dimensional metallic nature of $K_3Cu_8S_6$ and preliminary X-ray data, a second order reversible transition at $T_1=152\pm1K$ has been identified as the onset of an incommensurate lattice. In the region of 50-60K, a first order transition with considerable hysteresis seems to be a structural transition to a commensurate superlattice state.

20. DISTRIBUTION/AVAILABILITY OF ABSTRACT: ☒ UNCLASSIFIED/UNLIMITED ☒ SAME AS RPT ☐ DTIC USERS	21. ABSTRACT SECURITY CLASSIFICATION: UNCLASSIFIED
22a. NAME OF RESPONSIBLE INDIVIDUAL	22b. TELEPHONE (Include Area Code); 22c. OFFICE SYMBOL

(12)

OFFICE OF NAVAL RESEARCH

Contract N00014-86-K-0608

R&T Code 413a001---01

Technical Report No. 25

Charge Density Waves in the Mixed-Valence Two-Dimensional Metal, $K_3Cu_8S_6$

L. W. ter Haar, F. J. Di Salvo, H. E. Bair, R. M. Fleming, and J. V. Waszczak

AT&T Bell Laboratories
Murray Hill, New Jersey 07974

W. E. Hatfield
University of North Carolina
Department of Chemistry
Chapel Hill, North Carolina 27514

Prepared for Publication in Physical Review

87 1 01 104

CHARGE DENSITY WAVES IN THE MIXED-VALENCE TWO-DIMENSIONAL METAL, $K_3Cu_8S_6$

L. W. ter Haar, F. J. Di Salvo, H. E. Bair, R. M. Fleming and J. V. Waszczak*

AT&T Bell Laboratories
Murray Hill, New Jersey 07974

W. E. Hatfield

Department of Chemistry

University of North Carolina at Chapel Hill
Chapel Hill, North Carolina 27514

ABSTRACT

In order to study the physical properties of $K_3Cu_8S_6$, we have carefully defined the synthetic conditions for KCu_4S_3, $K_3Cu_8S_6$ and KCu_3S_2. $K_3Cu_8S_6$ is apparently a kinetic phase and must be trapped with a minimum amount of either KCu_4S_3 or KCu_3S_2. Magnetic susceptibility and electrical resistivity data display behavior typical of CDW systems. In view of the low-dimensional metallic nature of $K_3Cu_8S_6$ and preliminary X-ray data, a second order reversible transition at $T_1 = 152 \pm 1K$ has been identified as the onset of an incommensurate lattice. In the region of 50-60K, a first order transition with considerable hysteresis seems to be a structural transition to a commensurate superlattice state.

* Department of Chemistry, Baker Laboratory, Cornell University, Ithaca, New York 14853

CHARGE DENSITY WAVES IN THE MIXED-VALENCE TWO-DIMENSIONAL METAL, $K_3Cu_8S_6$

L. W. ter Haar, F. J. Di Salvo, H. E. Bair, R. M. Fleming and J. V. Waszczak*

AT&T Bell Laboratories
Murray Hill, New Jersey 07974

W. E. Hatfield

Department of Chemistry

University of North Carolina at Chapel Hill
Chapel Hill, North Carolina 27514

INTRODUCTION

Rudorff et al[1] first reported the existence of the composition $K_3Cu_8S_6$ as part of an investigation concerning the products of high temperature fusion reactions involving alkali carbonates, copper, and sulfur. Their results indicated that the new phases $Na_2Cu_3S_3$, KCu_4S_3, $RbCu_4S_3$ and $K_3Cu_8S_6$ all have metallic conductivity at room temperature (ca. 50-100 $\Omega^{-1}cm^{-1}$) in addition to a blue-black metallic lustre. Stimulated by the apparent "mixed valency" of the Cu (e.g., Cu^{+1} and Cu^{+2}) and the electrical conductivity of these compounds, several research groups have taken a closer look at the structural and physical properties of some of these materials.

The composition "$Na_2Cu_3S_3$" was reported by Rudorff[1] as the sole product of the fusion reaction between copper, sulfur, and sodium carbonate. More recent results by both Burschka[2] and Brown[3] have shown that this "$Na_2Cu_3S_3$" phase is actually $Na_3Cu_4S_4$, and can be described as a one-

---

* Department of Chemistry, Baker Laboratory, Cornell University, Ithaca, New York 14853

dimensional metal. The structure consists of one-dimensional columns of $[Cu_4S_4]^{3-}$ chains separated by sodium ions, and the physical properties are in agreement with metallic behavior.

Brown[4] has also reported single crystal X-ray diffraction results and physical properties for the KCu_4S_3 phase reported by Rudorff[1]. Their results indicate that KCu_4S_3 adopts a double layer structure (S-Cu-S-Cu-S) and exhibits metallic behavior. Therefore, KCu_4S_3 is a two-dimensional metal as opposed to the one-dimensional example provided by $Na_3Cu_4S_4$. Burschka[5] has reported the structure for $CsCu_4S_3$ and found it to be isotypic with KCu_4S_3 and $RbCu_4S_3$.

The first attempts by Burschka to synthesize $K_3Cu_8S_6$ were unsuccessful and led to the discovery of the as yet unknown compound KCu_3S_2 [6]. Interestingly, Burschka[5] has also found that $CsCu_3S_2$ exists, but that it adopts a new structure type which is totally unlike that of KCu_3S_2. In subsequent work, Burschka[7] succeeded in synthesizing $K_3Cu_8S_6$ and reported the results of a single crystal X-ray diffraction study. The synthetic conditions Burschka reported were, however, in conflict with those reported by Rudorff[1]. In a closely related study, Schils et al[8] have reported the synthesis and structure of the isotypic compounds $Rb_3Cu_8Se_6$ and $Cs_3Cu_8Se_6$.

Stimulated by the variety of compounds obtained from this series of alkali carbonate fusion reactions as well as the intriguing combination of unusual structure and metallic conductivity, we have reinvestigated the synthesis of

$K_3Cu_8S_6$ in order to investigate its physical properties. Both magnetic susceptibility and electrical resistivity measurements were made, and both show remarkably unusual behavior. Behavior which we feel is most likely attributable to the presence of a charge density wave (CDW).

Synthesis

There are three K-Cu-S phases which can be obtained from high temperature fusion reactions involving K_2CO_3, powdered copper, and elemental sulfur. Namely, these are KCu_4S_3 (or $K_2Cu_8S_6$), $K_3Cu_8S_6$, and KCu_3S_2 (or $K_3Cu_9S_6$). It is interesting to note at this point the stoichiometric relationship,

$$K_2Cu_8S_6 \xrightarrow{K} K_3Cu_8S_6 \xrightarrow{Cu} K_3Cu_9S_6 \qquad (1)$$

since there are also synthetic and structural trends which systematically vary from KCu_4S_3 to KCu_3S_2. Since there are discrepancies in the literature concerning the syntheses of these materials, we report our synthesis with some detail.

Rudorff[1] first reported that by reacting 6g potassium carbonate, 6g sulfur and 1g copper powder (K_2CO_3:S:Cu::2.8:1:12 molar ratios), KCu_4S_3 or $K_3Cu_8S_6$ can be obtained. By slowly heating to a specified temperature and soaking at that temperature for a specified time, either KCu_4S_3 (800 °C, 1 hr.) or $K_3Cu_8S_6$ (1000 °C, 3 hr.) can be the resultant product. The single crystal X-ray diffraction study by Brown[4] demonstrated that KCu_4S_3 can indeed be synthesized in this manner. However, any systematic attempts to change the procedure in order to improve crystal size or quality, were generally

unsuccessful. Burschka[6] was attempting to synthesize $K_3Cu_8S_6$ by Rudorff's method (1000°C, 3 hrs.) when he discovered the as yet unknown phase, KCu_3S_2. His final results indicated KCu_3S_2 was best synthesized in the temperature range 780°C-850°C with a one-hour soak period. His report simply concluded that at lower temperatures, both KCu_4S_3 and $K_3Cu_8S_6$ could be identified in powder X-ray diffraction patterns, but did not elaborate. In his later study, Burschka[7] reported that $K_3Cu_8S_6$ was indeed obtainable from a lower, but somewhat narrow temperature range. At 790°C he found that the formation of KCu_4S_3 and/or $K_3Cu_8S_6$ could be controlled by the length of the soak period. Specifically, two hours led to a product which yielded X-ray quality crystals of $K_3Cu_8S_6$.

In our own initial attempts to synthesize $K_3Cu_8S_6$, we actually synthesized several unwanted batches of either KCu_4S_3 or KCu_3S_2. $K_3Cu_8S_6$ would sometimes appear only as the minor second phase in a few of the multiphase batches. $K_3Cu_8S_6$ crystals are needlelike, and as such, are easy to separate from the layer-like crystals of KCu_4S_3. On the other hand, KCu_3S_2 crystals are also needlelike and for all practical purposes, indistinguishable from $K_3Cu_8S_6$. So, if a few X-ray quality sized crystals is all that is desired, the mixed phase system of $KCu_4S_3/K_3Cu_8S_6$ is the system of choice since the two materials can be easily distinguished from one another. However, in order to obtain bulk single phase $K_3Cu_8S_6$ product, and in order to clarify the discrepancies in the literature, we have attempted to define the syntheses of these materials more precisely.

We initially held to Rudorff's prescribed amounts of starting material (6g K_2CO_3, 6g, S, 1g Cu) since we felt the large excess of potassium and sulfur was necessary to provide a growth medium for the crystals (a hypothesis later verified by experiments discussed below). The starting materials were ground together and placed into an alumina crucible which was deep enough to contain the initial bubbling (foaming) which occurs upon heating. The crucible was covered with a [illegible] alumina cap, and then placed inside a long and deep carbon crucible. This carbon crucible was then placed inside a vertical quartz tube which was contained inside a vertical tube furnace. Without the graphite crucible, K_2CO_3 vapor attacked the quartz tube irreversibly. Provisions at the top of the quartz tube allowed the system to be sealed off with an inert gas flow (Argon) and the insertion of a thermocouple down to the reaction zone. The quartz vessel was long enough such that some of it was exposed to room temperature air in order to keep it cool enough so that excess sulfur would condense on the quartz walls and not inside the gas-flow tubing (where blockage could occur).

After sufficient flushing of the reaction vessel with the argon, a small flow rate of argon (1 bubble/sec in oil bubbler) was maintained throughout the reaction process. Figure 1 is a plot of our synthesis results in terms of set-point temperature vs. soak period. The heating rate from room temperature to the set point was 125 °C/hr. To cool the reaction, the furnace was simply shut off at the end of the soak period and allowed to cool down at a rate of ca. 125 °C/hr. Fig. 1 demonstrates the relationship we began to notice after several

runs. In general, KCu_4S_3 and KCu_3S_2 are the predominant phases in this reaction system. The lower temperature phase is KCu_4S_3, and the higher temperature phase is KCu_3S_2. The boundary between these two phases varies from approximately 900 °C to 800 °C, depending on the length of the soak period. Clean material of either KCu_4S_3 or KCu_3S_2 can be made by using reaction conditions well removed from the boundary lines as indicated in Fig. 1. In between the boundary lines is where $K_3Su_3S_6$ can be found as a product. The data in Fig. 1 indicate that a shorter soak period and higher soak temperature favor the formation of $K_3Cu_8S_6$. For soak periods of 5 hours or longer, $K_3Cu_8S_6$ is hardly detectable in X-ray powder patterns since the boundary between KCu_4S_3 and KCu_3S_2 apparently becomes more crisply defined. The optimum conditions for synthesizing $K_3Cu_8S_6$ seem to be a soak temperature of 875 °C for a 1-2 hour period. Shorter than one hour, and the product is neither crystalline nor clean in terms of its X-ray powder diffraction pattern. Finally, the last parameter which we found to affect the reaction product was the particle size of the K_2CO_3. The data in Fig. 1 are for well ground materials. If coarser K_2CO_3 was used, the effective boundary line shifted to a higher temperature and/or a longer time. We interpret this as a result of the kinetics of K_2CO_3 decomposition and its reaction with sulfur. Smaller K_2CO_3 particles simply allow for faster kinetics due to their increased surface area with respect to larger particles. Since the formation of $K_3Cu_8S_6$ is sensitive towards the reaction time and temperature, it is actually not surprising that the K_2CO_3 particle size would also have a pronounced effect on $K_3Cu_8S_6$

formation. By all evidence, $K_3Cu_8S_6$ seems to be a kinetic phase (i.e., non-equilibrium) and as such, must be "trapped" under the best available conditions. Our cleanest product was greater than ~95% pure $K_3Cu_8S_6$. The small amount of KCu_4S_3 was easily recognizable (platelets) and manually separated from the $K_3Cu_8S_6$ crystals.

The actual workup of the cooled cake is straightforward. Since the cooled cake is usually firmly stuck in the alumina crucible, it is filled with a deoxygenated 50:50 mixture of ethanol/distilled water to leach out the soluble polysulfides. The yellow solution is decanted off after some time is allowed for the leaching to occur (ultrasonic agitation helps), and then the process is repeated. When the solution becomes colorless and odorless, the leaching process is complete and shiny blue-black crystals should be all that remain. After suction filtering the crystals under an argon flow, they are washed with absolute ethanol and anhydrous ethyl ether. The crystals can then be thoroughly dried under vacuum. $K_3Cu_8S_6$ crystals are needlelike crystals that are similar in overall appearance to KCu_3S_2 crystals. KCu_4S_3 crystals form easily recognizable platelets. If $K_3Cu_8S_6$ crystals are left exposed to the atmosphere, they will lose their metallic lustre over the course of a few days due to oxidation reactions with moist air. Product batches were characterized by powder X-ray diffraction. Powder patterns for the pure materials are displayed in Fig. 2 and demonstrate that mixtures can be easily identified since many diffraction peaks do not overlap between the three phases. The relative purity of product batches was estimated from the diffraction pattern intensities as well

as by visible examination in the case of $KCu_4S_3/K_3Cu_8S_6$ mixtures.

RESULTS

Magnetism

Magnetic susceptibility data for $K_3Cu_8S_6$ were obtained using a cryogenically equipped Faraday Balance at an externally applied magnetic field of 10.6 kG and a gradient of 0.939 kG/cm[9]. The data are displayed in Fig. 3 using two different formats. The upper curve represents the experimentally observed gram susceptibility. The data were collected with the temperature decreasing as well as with the temperature increasing at rates of 0.5 to 1.0 K/min. The rising susceptibility at low temperatures in the upper curve is due to a Curie contribution from paramagnetic impurities. Hence, the data below 15K were fit to the form $\chi_0 + \frac{C}{(T+\Theta)}$, where χ_0 is assumed to be temperature independent and $\frac{C}{(T+\Theta)}$ accounts for the paramagnetic impurity ($C=3.573$, $\Theta=0$) and is subtracted out of the entire upper curve in Fig. 3 to yield the lower curve. The lower curve is assumed to be the intrinsic susceptibility and is the sum of the diamagnetic core contributions and the Pauli-Landau and Van-Vleck paramagnetic contributions. The magnetic susceptibility is only weakly temperature dependent above 180K, but shows a stronger temperature dependence indicative of phase transitions below 180K. There is a reversible transition (probably second order) at approximately 150K which is more clearly displayed in the derivative $d\chi_g/dT$ as shown in Fig. 4. The curve for $d\chi_g/dT$ is obtained by fitting the observed χ_g data to a quadratic polynomial for every eight consecutive data points. The linear coefficient is then extracted and

plotted versus temperature to yield the $d\chi_g/dT$ vs. T curve. In the region of 50K there is a first order transition with considerable hysteresis. A pretransition "dip" in the susceptibility appears at about 60-65K in the cooling curves, but not in the heating curve.

Conductivity

Temperature dependent electrical resistivity measurements were made using the single crystal, four probe method. A typical crystal of dimensions 0.15mm×0.15mm×2.0mm was mounted with ultrasonic indium solder to four gold leads along the needle axis (b-axis). Initially, conducting silver epoxy was used for contacts, but these were found to react (perhaps $Ag^+ \leftrightarrow Cu^+$ ion exchange with the crystal) and the contact resistance became quite large after several hours.. The room temperature resistance of the crystal was measured as 0.24 Ω. The distance between the two voltage contacts measured approximately 1mm, and hence, the room temperature resistivity can be calculated to be 5×10^{-4} Ω·cm. An uncertainty of ±30% is estimated from the size of the contacts and the irregular crystal shape. The crystal exhibited ohmic behavior at room temperature, as well as stability of the contact resistance over the course of days.

Temperature dependence of the observed resistance of the crystal is plotted in Fig. 5 for the range 5-350K. The resistance decreases with decreasing temperature, indicative of metallic behavior down to ca. 160K. There is a reversible phase transition at ca. 150K which corresponds well with the phase

transition observed at 152±1K in the magnetic susceptibility. Upon further cooling, the resistance rises until ca. 63K, where there is a small dip in the resistance, just as there is in the magnetic susceptibility. Further cooling shows a dramatic decrease in resistance and leads to a state which is again metallic in the region of 5-50K. The heating curve demonstrates that a considerable hysteresis exists and that it extends up to at least 100K. As in the case of the magnetic susceptibility, the heating curve does not display the anomaly near 63K. Fig. 6 shows dR/dT versus temperature and again shows that the second order phase transition occurs at about 152K. As in the case of the magnetic susceptibility, the derivative was obtained by fitting the experimental data to a quadratic polynomial for every eight consecutive points, and extracting the linear coefficient as the slope.

Specific Heat

The specific heat of $K_3Cu_3S_6$ was measured[10] in the temperature range of 100K to 300K. The specific heat shows no unusual behavior down to 160K, and is almost constant. As shown in Fig. 7, there is a small peak in the region of 150K, and both heating and cooling runs gave the same curve. This corresponds to the reversible phase transition seen in both the magnetic susceptibility and the electrical resistivity. The slope of the specific heat is more positive below the transition region than above the transition region.

Discussion

A relatively large number of copper-sulfide phases are known and most contain discrete oxidation (valence) states[4]. The major exception is the $Cu_{2-x}S$ ($0 \leq x \leq 0.2$) binary system where a variety of nonstoichiometric, "mixed-valence" phases can be found. An additional exeption lies in the K-Cu-S system, of which $K_3Cu_8S_6$, KCu_4S_3, and KCu_3S_2 are members, but only $K_3Cu_8S_6$ and KCu_4S_3 provide mixed-valence examples.

Although it is tempting to describe copper-sulfur mixed-valence compounds as $Cu^{I}Cu^{II}$ systems, most of the available evidence suggests that the mixed-valency resides primarily on the sulfur and not on the copper[11-13]. X-ray photoelectron spectroscopy suggests that all known copper sulfides (including $Cu_{2-x}S$, KCu_4S_3, and $Na_3Cu_4S_4$) contain only Cu(I). There is no direct evidence to date that shows that Cu(II) or intermediate oxidation states exist in these copper-sulfide phases. With these results in mind, the mixed-valency in KCu_4S_3 might be formulated as $K^{+}\,Cu_4^{+}\,(S^{2-})_2S^{-}$. Similarly, another example is provided by $Na_3^{+}\,Cu_4^{+}\,(S^{2-})_3S^{-}$ in $Na_3Cu_4S_4$. As such, we can formulate $K_3Cu_8S_6$ as a Robin and Day[14] class IIIB mixed-valence material with the formula $K_3^{+}\,Cu_8^{+}\,(S^{2-})_5S^{-}$. These ionic like notations are useful primarily for descriptive purposes and are consistent with results from photoelectron spectroscopy of copper sulfides. However, it is clear that covalency is very important in these phases, and it is likely that the wavefunctions at the Fermi surface of these metallic compounds have considerable copper as well as sulfur character.

As a class IIIB mixed valence material, $K_3Cu_8S_6$ could be expected to show metallic behavior. The electrical resistivity results confirm this with a drop in resistivity of approximately two orders of magnitude from 300K to 5K. The absolute value of the resistivity ($\rho(300K) \cong 5 \times 10^{-4} \Omega cm$) is similar in value to other metallic phases with layered structures[15].

From a structural point of view, $K_3Cu_8S_6$ is also an interesting material. The crystal structures of KCu_4S_3, $K_3Cu_8S_6$, and KCu_3S_2 are shown in Fig. 8. The low temperature phase KCu_4S_3 is a close packed double-layered structure (S-Cu-S-Cu-S) in which all copper ions are tetrahedrally coordinated[4]. The high temperature phase, KCu_3S_2, is also a layered structure but has a pleated character because the copper ions are in both tetrahedral and trigonal coordination sites[6]. A remarkable feature of KCu_3S_2 is that $^1_\infty[Cu_4S_4]^{n-}$ chains are bridged by edge-sharing tetrahedra to yield the pleated layers, which are separated by potassium ions. The structure of $K_3Cu_8S_6$ is intermediate between that of KCu_4S_3 and KCu_3S_2 [7]. It is not surprising then that the $K_3Cu_8S_6$ synthesis conditions are "intermediate" between the syntheses of KCu_4S_3 and KCu_3S_2. Additionally, the stoichiometric sequence

$$K_2Cu_8S_6 \xrightarrow{K} K_3Cu_8S_6 \xrightarrow{Cu} K_3Cu_9S_6 \qquad (2)$$

also suggests that $K_3Cu_8S_6$ might be an intermediate structure.

$K_3Cu_8S_6$ is most like KCu_3S_2 in that the $^1_\infty[Cu_4S_4]^{n-}$ chain is an integral part of the layer structure. Fig. 9 schematically demonstrates how this vital part of $K_3Cu_8S_6$ is based upon trigonal coordination of the copper ions. These

resultant $^1_\infty[Cu_4S_4]^{n-}$ chains are bonded into layers using edge sharing tetrahedra that resemble a small segment of half of the double layer found in the KCu_4S_3 structure. The crystal structure report by Burschka shows that the Cu3 ions, which are the heart of this bridging network between $^1_\infty[Cu_4S_4]^{n-}$ chains, have either a large amount of thermal motion or a slight disorder[7]. (This is indicated in Fig. 8 by the elliptical shapes assigned to the Cu3 ions.) It is interesting to note at this point that the idea of a $^1_\infty[M_4S_4]^{n-}$ chain is also evident in other structures. Fig. 10 demonstrates that $Na_3Cu_4S_4$ and $K_2Ag_4S_3$ also possess this columnar chain as the fundamental unit of their solid state structure. It is clearly the manner in which this columnar chain packs into the lattice that is responsible for the overall differences in structure. In the case of $K_3Cu_8S_6$ (as well as the others) the packing of these $^1_\infty[Cu_4S_4]^{n-}$ chains into layers results in layers which have an anisotropic character, unlike the more conventional layered materials such as $NbSe_2$, TaS_2, etc.

The electrical resistivity and magnetic susceptibility for $K_3Cu_8S_6$ clearly show the presence of phase transitions in the region of 55K and 150K. The most likely explanation for the observed behavior in $K_3Cu_8S_6$ is the presence of a charge density wave (CDW). Charge density waves are most common in lower-dimensional materials (metals) such as $NbSe_3$ (one-dimensional) and $TaSe_2$ (two-dimensional) but are occasionally seen in three-dimensional materials such as CuV_2S_4 [16]. The simplest models suggest that CDW formation is favored in low-dimensional metals because anisotropic Fermi surfaces with regions of low-curvature are expected to occur, while in three-

dimensional materials such occurrences are "accidental"[17]. $K_3Cu_8S_6$ is clearly a lower-dimensional metal. However, the layers of $K_3Cu_8S_6$ have an anisotropic two-dimensional character because of the manner in which the layers are composed of chains. The crystal dimensions were too small to obtain a measure of the electrical in-layer anisotropy, but the retention of metallic behavior below the transitions suggests that the anisotropy is not large enough to make the system quasi-one-dimensional. Such large anisotropies do exist in some structurally two dimensional metals so that the CDW properties are effectively one-dimensional (for example, in $K_{0.3}MoO_3$)[18]. Since $K_3Cu_8S_6$ meets the structural criteria and can be considered a low-dimensional metal, CDW formation is a likely explanation for the observed magnetic susceptibility and electrical resistivity based on the similar behavior of precedent systems[17]. In particular, the observed behavior of $K_3Cu_8S_6$ is very similar to CuV_2S_4 [16]. The major difference is the enhanced value of the magnetic susceptibility in CuV_2S_4 due to electron-electron interactions, as well as the actual temperatures of the transitions. The magnitude of the relative behavior in terms of changes in susceptibility at the phase transitions is, however, very similar between $K_3Cu_8S_6$ and CuV_2S_4. However, observation of an incommensurate lattice modulation in a metal is what is really needed in order to show CDW formation. Our preliminary low temperature single crystal X-ray diffraction results do indeed indicate that the phase transition at 153K produces an incommensurate state with a wave vector $\vec{q} = (1-\delta)\,\vec{b}^*/2$ where $\delta(150K) \simeq 0.1$ (note that $\vec{b}^*$ is parallel to $\vec{b}$, which lies along the needle axis). The distortion becomes

commensurate at the first-order transition near 55K. This structural data coupled with the physical properties strongly suggest CDW formation in $K_3Cu_8S_6$. Further X-ray work is in progress and will be reported later.

Conclusion

We have refined and explained the previously confusing synthesis of the interesting structure $K_3Cu_8S_6$. Based on structural similarities to KCu_4S_3 and KCu_3S_2, we conclude that $K_3Cu_8S_6$ is a kinetic phase which must be carefully "trapped". Investigation of the electrical resistivity and magnetic susceptibility has led us to suggest that CDW formation is responsible for the phase transitions in $K_3Cu_8S_6$. Based on the mixed valency (e.g., metallic properties) and the low-dimensional structure of $K_3Cu_8S_6$, CDW formation is indeed likely. X-ray results confirm the presence of an incommensurate lattice below 150K. Future results will be reported on in order to structurally describe the CDW phenomena in $K_3Cu_8S_6$.

Acknowledgements

We would like to acknowledge our former colleague, D. B. Brown, who originally brought the K-Cu-S systems to our attention at both the University of North Carolina at Chapel Hill and AT&T Bell Laboratories prior to his death.

REFERENCES

[1] W. Rudorff, H. G. Schwarz, M. Walter, *Z. Anorg. Allg. Chemie, 269,* 141 (1952).

[2] C. Burschka, *Z. Naturforsch., 34b,* 396 (1979).

[3] Z. Peplinski, D. B. Brown, T. Watt, W. E. Hatfield, P. Day, *Inorg. Chem., 21,* 1752 (1982).

[4] D. B. Brown, J. A. Zubieta, P. A. Vella, J. T. Wrobleski, T. Watt, W. E. Hatfield, P. Day, *Inorg. Chem., 19,* 1945 (1980).

[5] C. Burschka, *Z. Anorg. Allg. Chem., 463,* 65 (1980).

[6] C. Burschka, W. Bronger, *Z. Naturforsch., 32b,* 11 (1977).

[7] C. Burschka, *Z. Naturforsch., 34b,* 675 (1979).

[8] H. Schils, W. Bronger, *Z. Anorg. Allg. Chemie, 456,* 187 (1979).

[9] F. J. Di Salvo, S. A. Safran, R. C. Haddon, J. V. Waszczak, *Phys. Rev. B20,* 4883 (1979).

[10] F. S. Bates, H. E. Bair, M. A. Hartney, *Macromolecules, 17,* 1987 (1984).

[11] J. C. W. Folmer, Thesis, University of Groningen, 1981.

[12] J. C. W. Folmer, F. Jellinek, *J. Less-Common Met., 76,* 153 (1980).

[13] C. F. van Bruggen, *Ann. Chim. Fr., 7,* 171 (1982).

[14] M. B. Robin and P. Day, *Adv. Inorg. Chem. Radiochem., 10,* 248 (1967).

[15] See for example, F. J. Di Salvo and T. M. Rice, in *Physics Today,* April (1979).

[16] R. M. Fleming, F. J. Di Salvo, R. J. Cava, J. V. Waszczak, *Phys. Rev. B24,* 2850 (1981).

[17] F. J. Di Salvo, in *Electron-Phonon Interactions and Phase Transitions.* T. Riste, ed., Plenum, New York, NY, 1977, p. 107.

[18] L. F. Schneemeyer, F. J. Di Salvo, R. M. Fleming, and J. V. Waszczak, *J. Solid State Chem., 54,* 358 (1984).

FIGURE CAPTIONS

Fig. 1 By plotting the reaction soak period vs. soak temperature, the observed trend becomes self-evident. The cleanest $K_3Cu_8S_6$ can be isolated around 875 ° C and 1-2 hours. The area between the two dashed lines indicates the conditions under which at least some $K_3Cu_8S_6$ can be observed along with either KCu_4S_3 or KCu_3S_2.

Fig. 2 Powder X-ray diffraction patterns for KCu_4S_3, $K_3Cu_8S_6$ and KCu_3S_2. KCu_4S_3: tetragonal, a=3.899 Å , c=9.262 Å . $K_3Cu_8S_6$: monoclinic, a=17.332 Å , b= 3.83 Å , c=9.889 Å , β=104.12 ° . KCu_3S_2: monoclinic, a=14.773 Å , b=3.946 Å , c=8.182 Å , β=113.5 ° .

Fig. 3 Magnetic susceptibility data for $K_3Cu_8S_6$. Upper curve is the experimentally observed data during cooling and heating. The lower curve is the cooling data minus an impurity Curie term.

Fig. 4 Magnetic susceptibility derivative $d\chi_g/dT$ obtained by numerically differentiating the corrected susceptibility. The peak at 152±1K indicates a second-order, reversible transition.

Fig. 5 Temperature dependence of the experimentally observed resistance for a single crystal of $K_3Cu_8S_6$. The room temperature resistance of 0.24 Ω corresponds to a resistivity of $5\times10^{-4}\Omega$ cm (±30%).

Fig. 6 The derivative dR/dT plotted as a function of temperature demonstrates the existence of the second order phase transition at 153K as well as the broad hysteresis due to the first order transition.

Fig. 7 Specific heat data for $K_3Cu_8S_6$ display a reversible anomaly near 150K.

Fig. 8 Representations of the structures of KCu_4S_3, $K_3Cu_8S_6$ and KCu_3S_2. In $K_3Cu_8S_6$, note how Cu1, Cu3, S1 and S3 form a small segment of half of the double layer found in KCu_4S_3, while Cu2, Cu4, S2 and S3 form the $^1_\infty[Cu_4S_4]^{n-}$ component of the layered structure. In all cases, the potassium ions separate the layered structures.

Fig. 9 Schematic representation of how the vital $^1_\infty[Cu_4S_4]^{n-}$ structure is obtained from trigonally coordinated copper ions. The sheet of trigonally coordinated copper on the left is wrapped around (so that dashed lines meet) to yield the columnar chain structure on the right.

Fig. 10 Structures for $Na_3Cu_4S_3$ and $K_2Ag_4S_3$. The views down the b-axes ($^1_\infty[Cu_4S_4]^{n-}$ chain axis) demonstrate the similarity to the K-Cu-S systems.

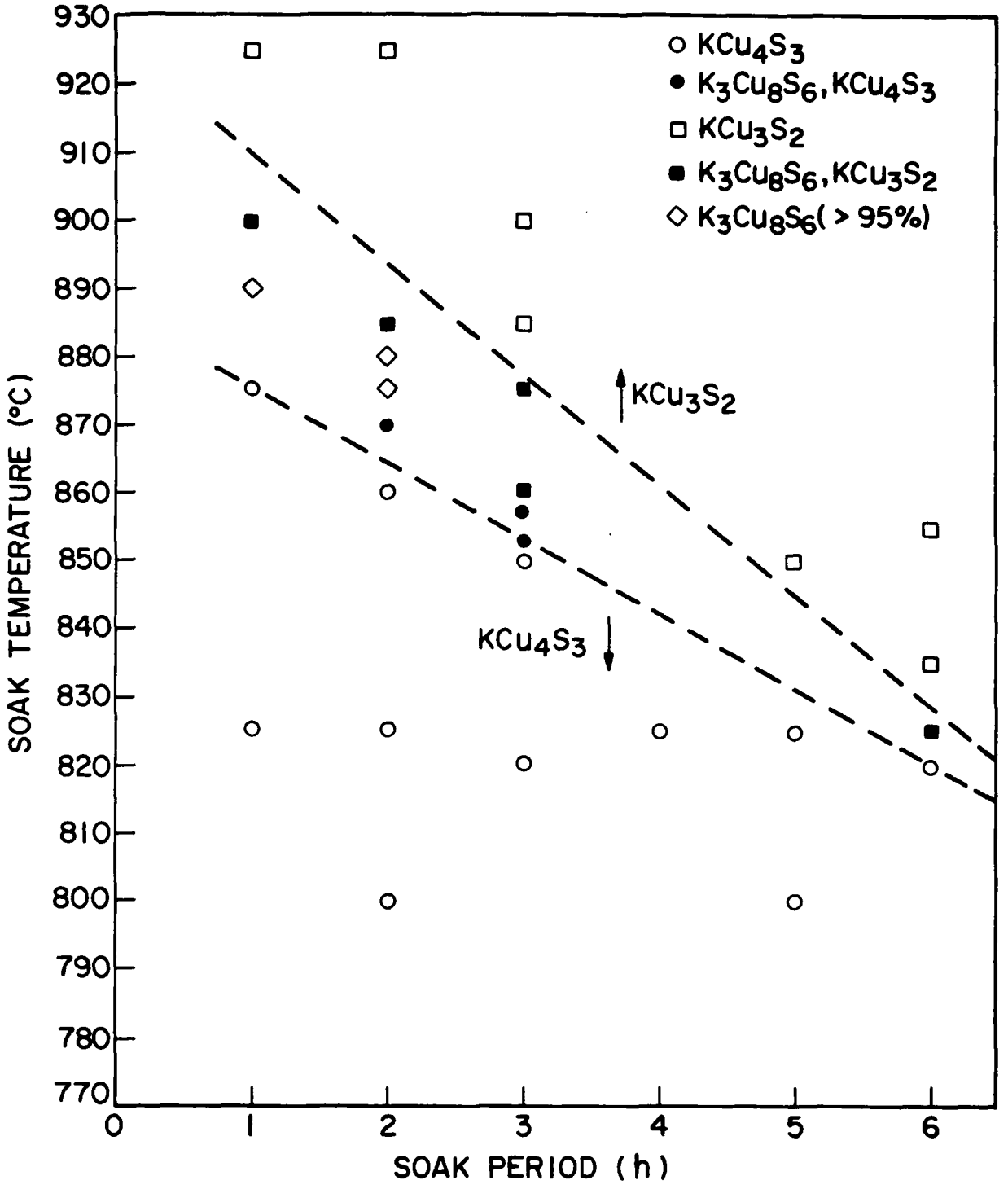

Fig 1

ter Haar et al PRB BT3183

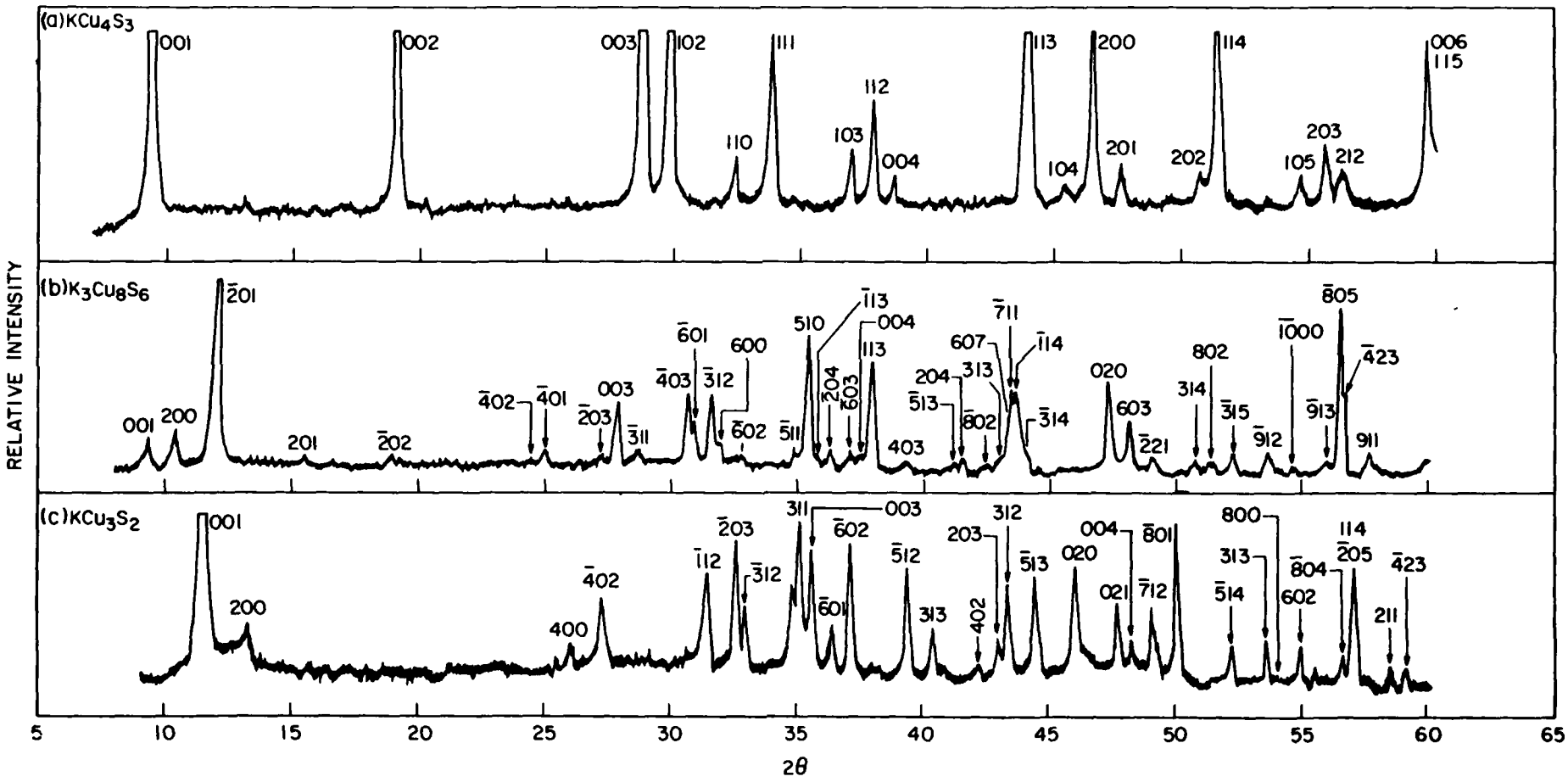
(a)KCu4S3
001
002
003
102
111
110
103
112
004
113
200
104
201
202
114
105
203
212
006
115
(b)K3Cu8S6
$\bar{2}01$
001
200
201
$\bar{2}02$
$\bar{4}02$
$\bar{4}01$
$\bar{2}03$
003
$\bar{3}11$
$\bar{4}03$
$\bar{6}01$
$\bar{3}12$
600
$\bar{6}02$
$\bar{5}11$
510
$\bar{1}13$
004
204
$\bar{6}03$
113
403
$\bar{5}13$
204
313
$\bar{8}02$
607
$\bar{7}11$
$\bar{1}14$
$\bar{3}14$
020
603
$\bar{2}21$
314
802
$\bar{3}15$
$\bar{9}12$
$\bar{1}000$
$\bar{9}13$
$\bar{8}05$
$\bar{4}23$
911
(c)KCu3S2
001
200
400
$\bar{4}02$
$\bar{1}12$
$\bar{2}03$
$\bar{3}12$
311
003
$\bar{6}02$
$\bar{6}01$
$\bar{5}12$
313
203
312
402
$\bar{5}13$
020
004
021
$\bar{8}01$
$\bar{7}12$
800
313
$\bar{5}14$
$\bar{8}04$
602
114
$\bar{2}05$
211
$\bar{4}23$
RELATIVE INTENSITY
5
10
15
20
25
30
35
40
45
50
55
60
65
2θ

Fig 2

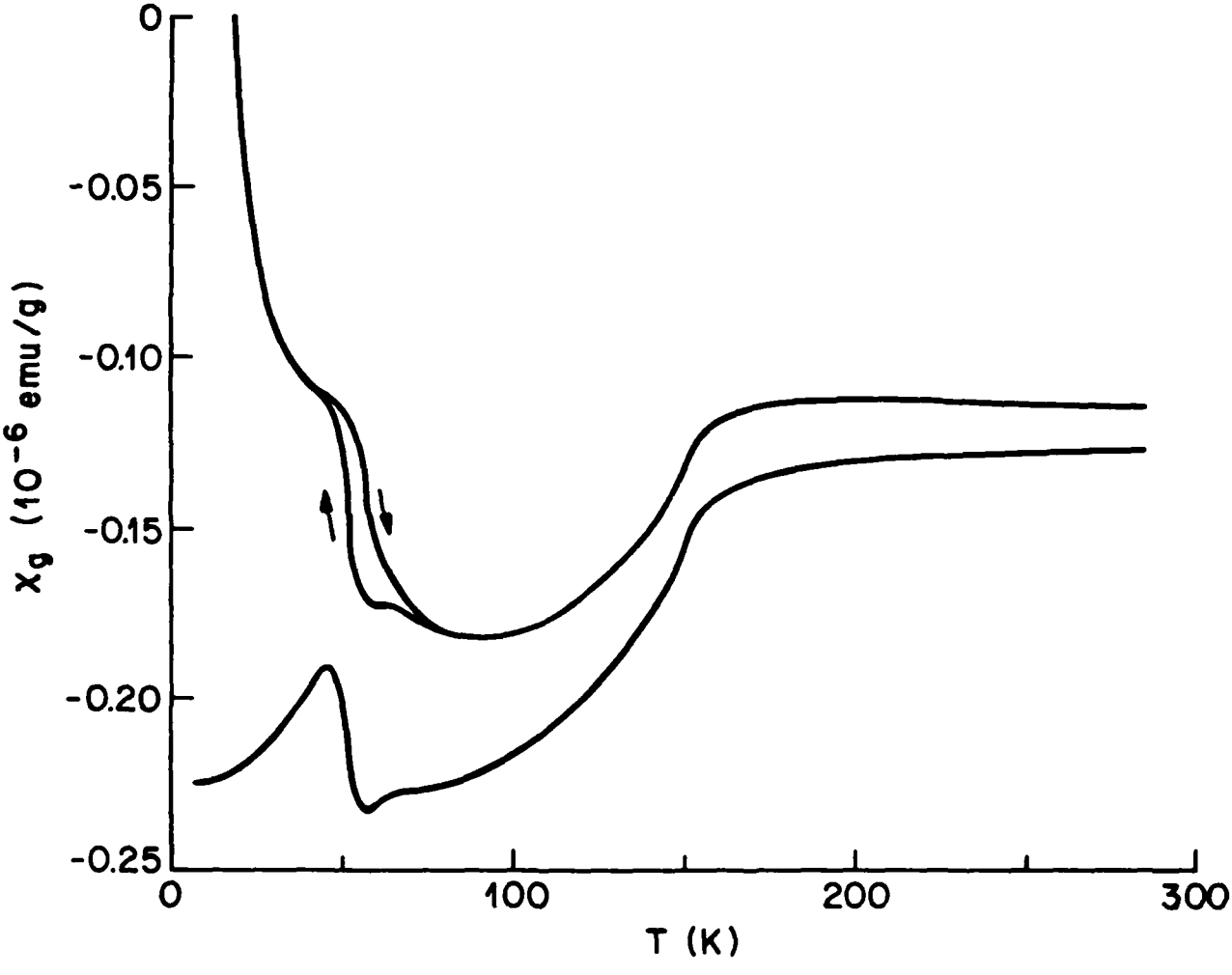

Fig 3

Hor et al PRB 6T3183

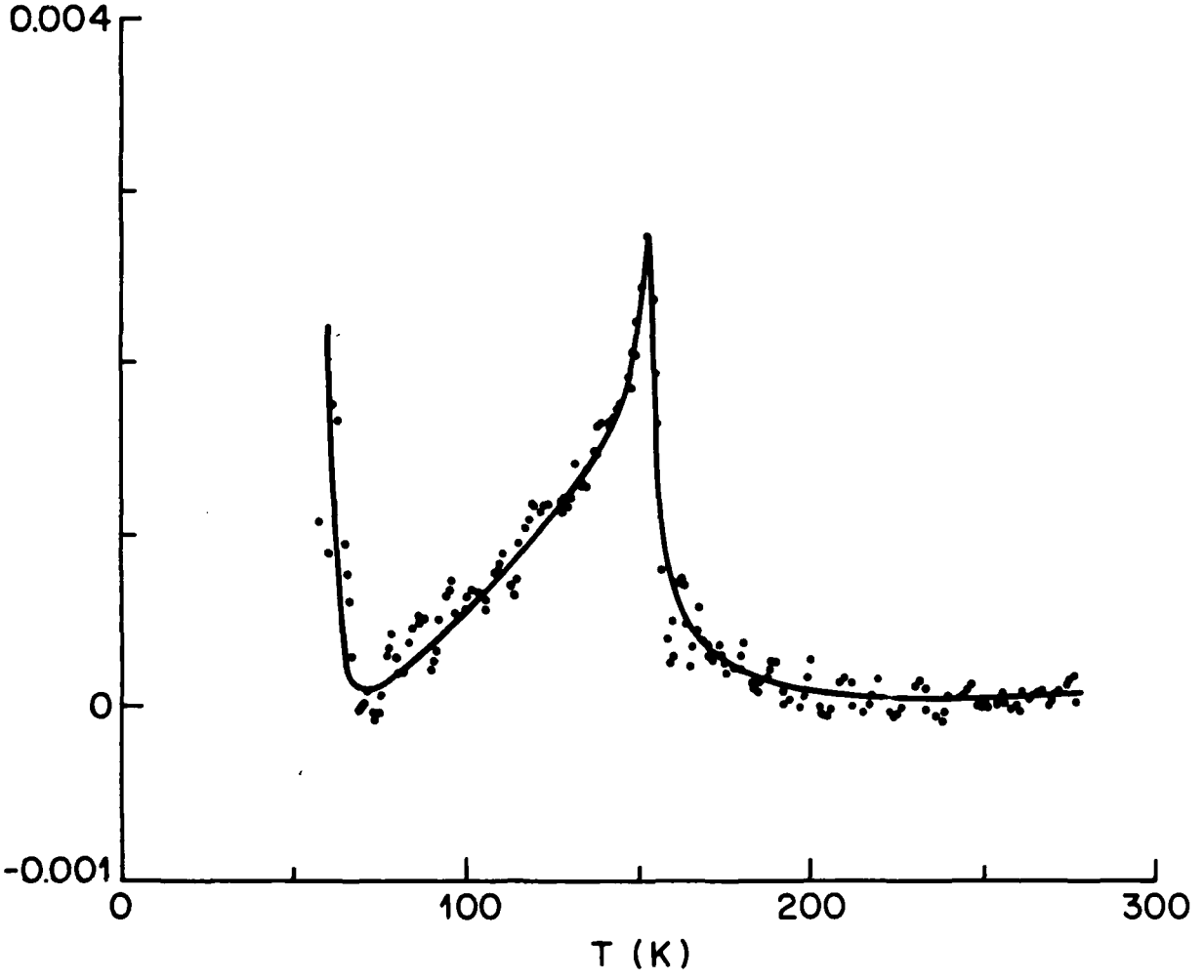

Fig 4

Haar et al_ PRB BT.3183

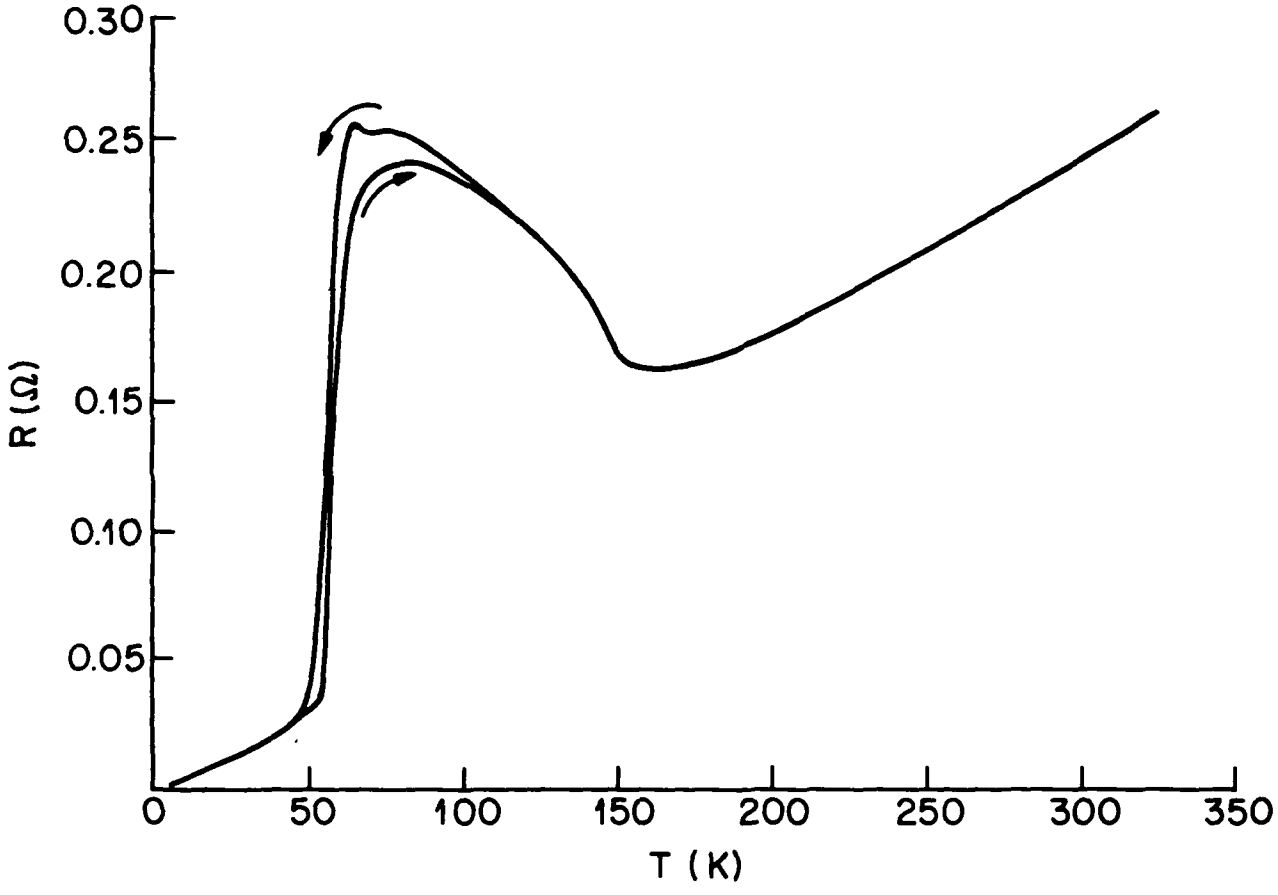

fig 5

Haar et al PRB

B7315 3

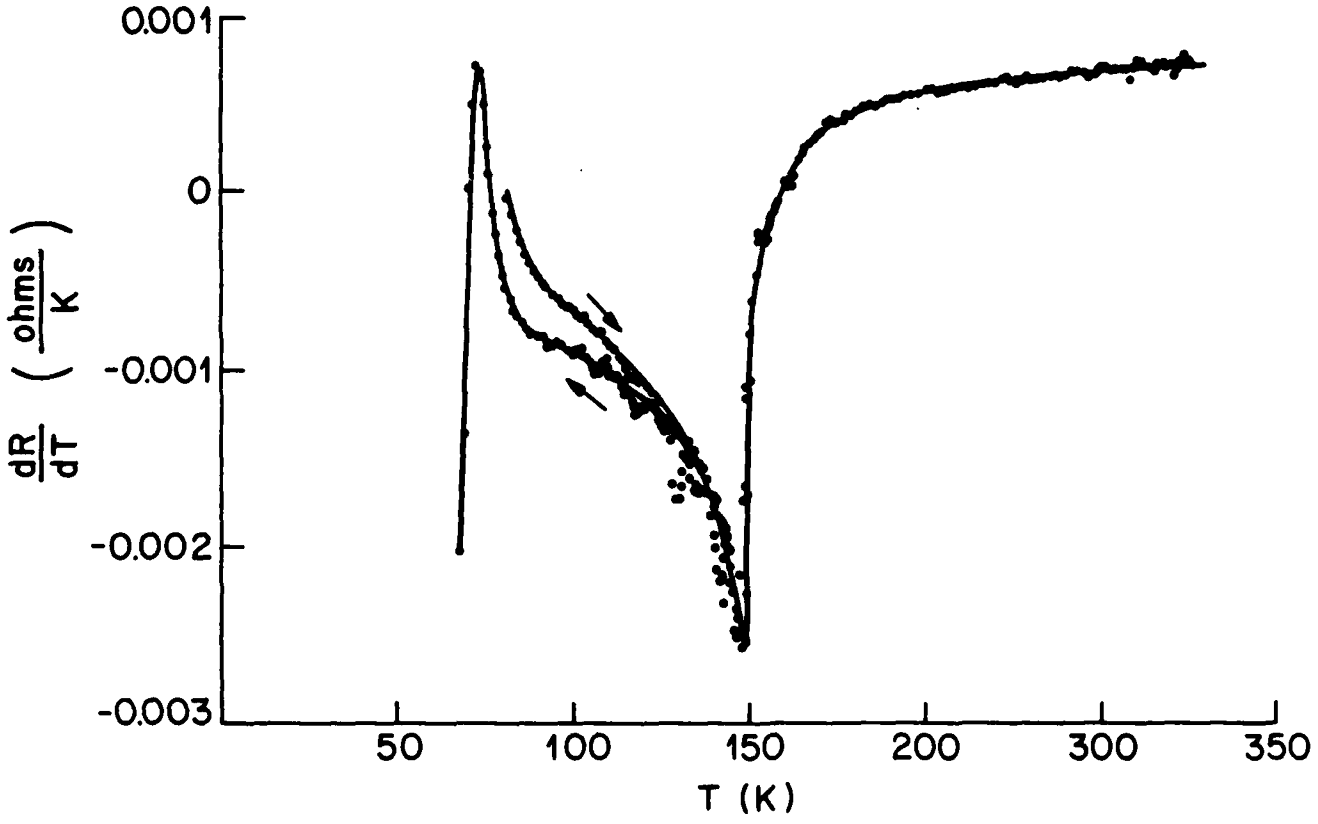

Fig 6

r Haar et al

<?TB/83

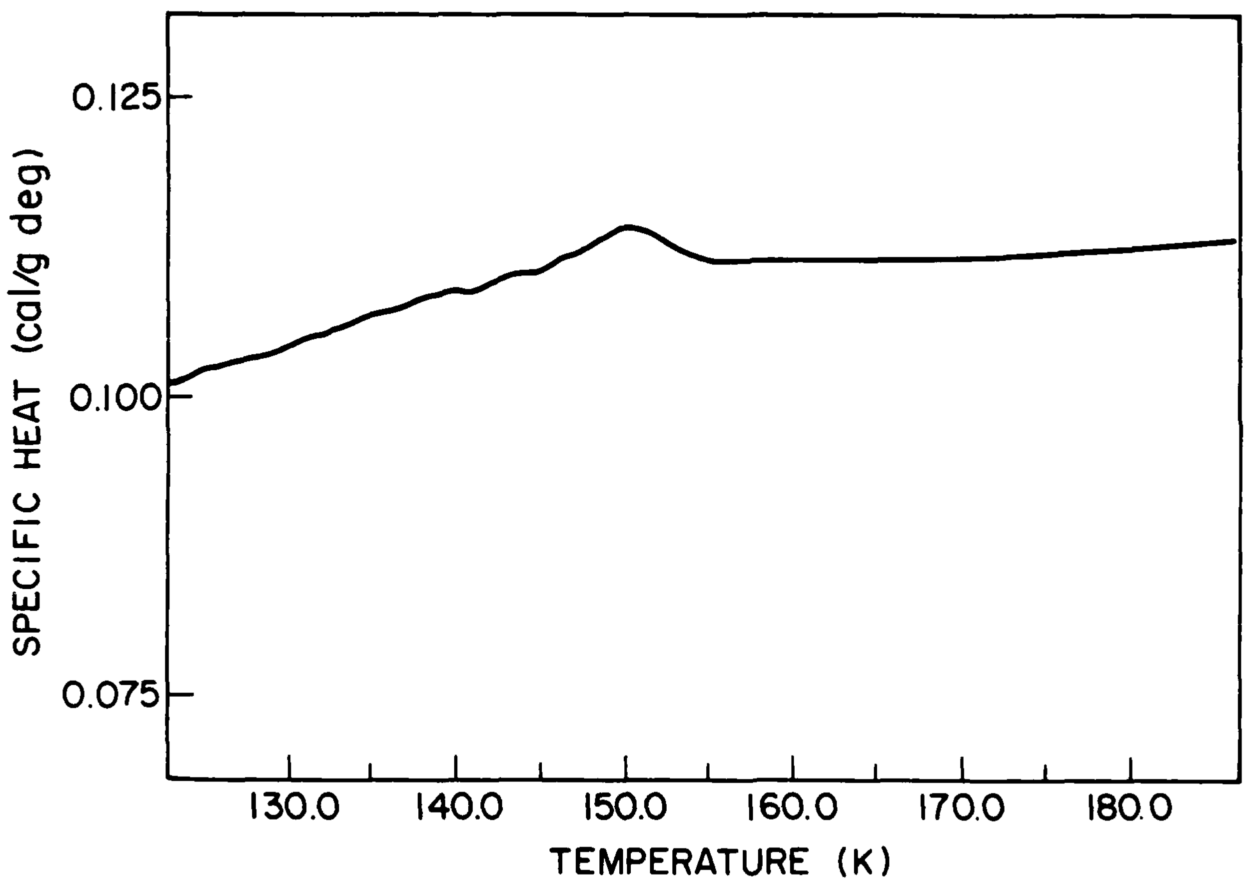

Fig 7

Haller et al PRB 13R3183

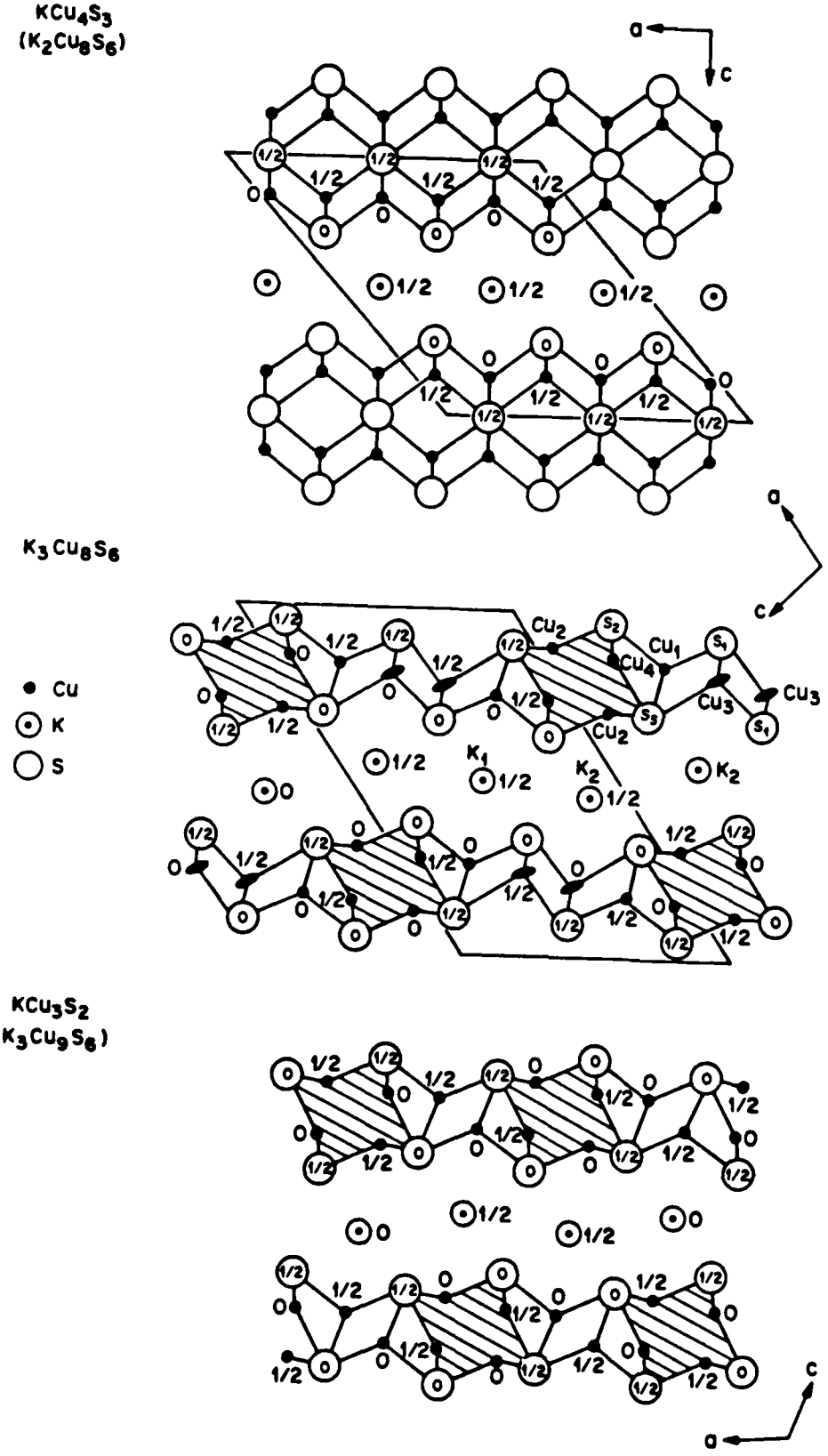

Hoard et al. PRB 6/3/83 Fig 8

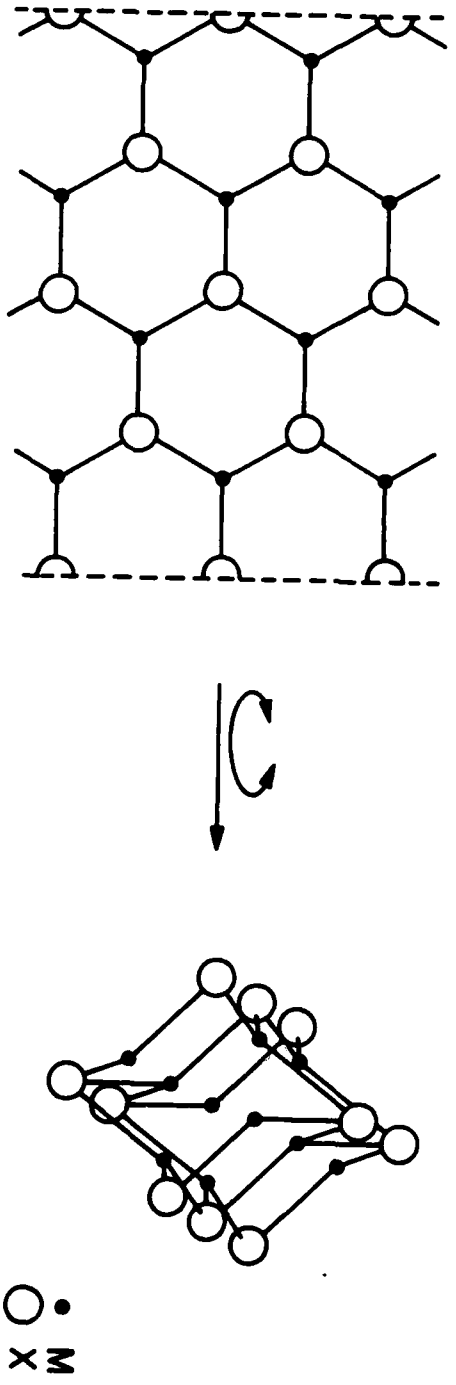

fig 9

ter Haar et al P11B B-3183

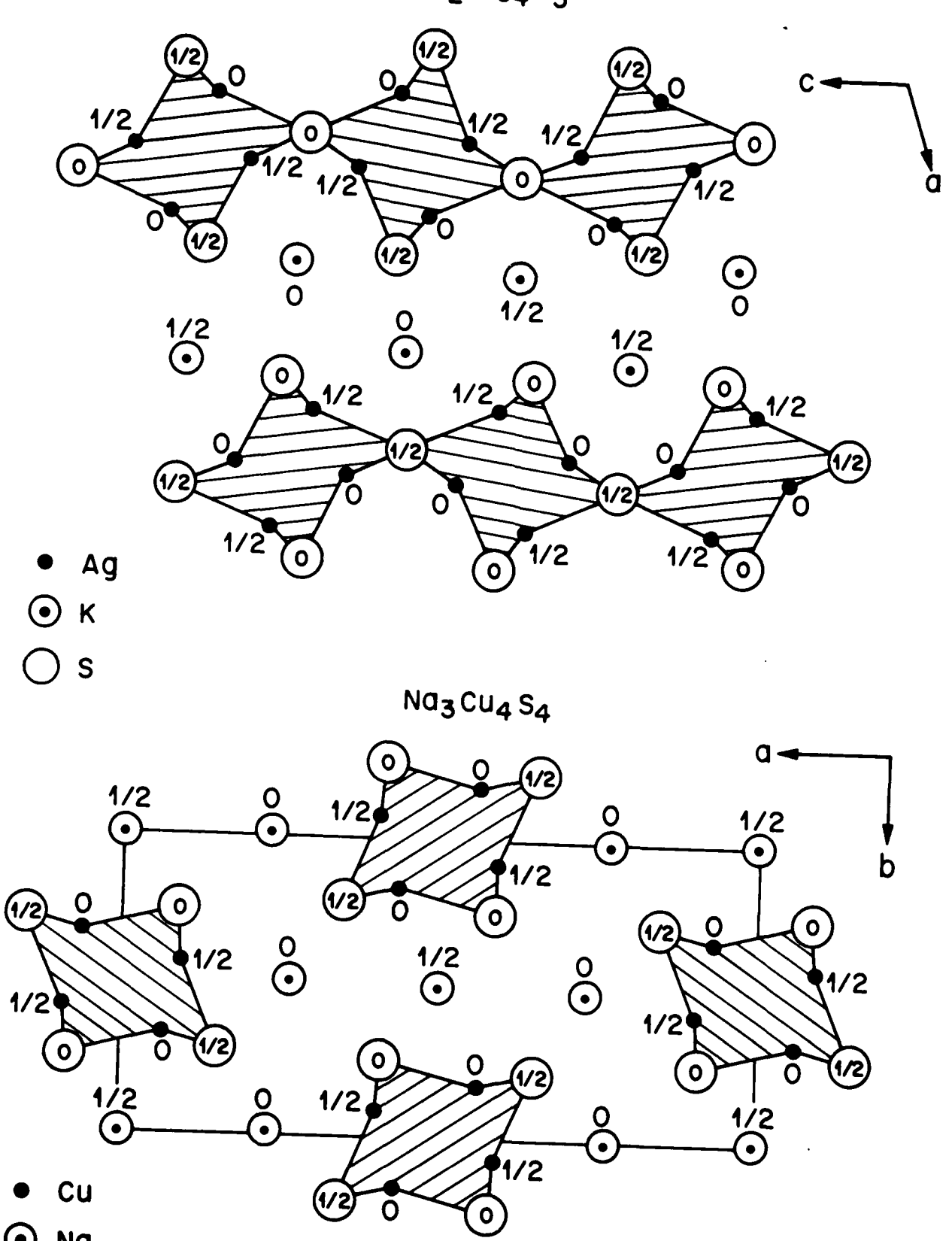

- Haar et al PRB 33 3183 fig 10

TECHNICAL REPORT DISTRIBUTION LIST, GEN

	No. Copies
Office of Naval Research Attn: Code 1113 800 N. Quincy Street Arlington, Virginia 22217-5000	2
Dr. Bernard Douda Naval Weapons Support Center Code 50C Crane, Indiana 47522-5050	1
Naval Civil Engineering Laboratory Attn: Dr. R. W. Drisko, Code L52 Port Hueneme, California 93401	1
Defense Technical Information Center Building 5, Cameron Station Alexandria, Virginia 22314	12 high quality
DTNSRDC Attn: Dr. H. Singerman Applied Chemistry Division Annapolis, Maryland 21401	1
Dr. William Tolles Superintendent Chemistry Division, Code 6100 Naval Research Laboratory Washington, D.C. 20375-5000	1
Dr. David Young Code 334 NORDA NSTL, Mississippi 39529	1
Naval Weapons Center Attn: Dr. Ron Atkins Chemistry Division China Lake, California 93555	1
Scientific Advisor Commandant of the Marine Corps Code RD-1 Washington, D.C. 20380	1
U.S. Army Research Office Attn: CRD-AA-IP P.O. Box 12211 Research Triangle Park, NC 27709	1
Mr. John Boyle Materials Branch Naval Ship Engineering Center Philadelphia, Pennsylvania 19112	1
Naval Ocean Systems Center Attn: Dr. S. Yamamoto Marine Sciences Division San Diego, California 91232	1

ABSTRACTS DISTRIBUTION LIST, 053

Dr. M. F. Hawthorne
Department of Chemistry
University of California
Los Angeles, California 90024

Professor O. T. Beachley
Department of Chemistry
State University of New York
Buffalo, New York 14214

Dr. W. Hatfield
Department of Chemistry
University of North Carolina
Chapel Hill, North Carolina 27514

Professor R. Wells
Department of Chemistry
Duke University
Durham, North Carolina 27706

Professor K. Neidenzu
Department of Chemistry
University of Kentucky
Lexington, Kentucky 40506

Dr. Margaret C. Etter
Department of Chemistry
University of Minnesota
Minneapolis, MN 55455

Dr. Herbert C. Brown
Department of Chemistry
Purdue University
West Lafayette, IN 47907

Dr. J. Zuckerman
Department of Chemistry
University of Oklahoma
Norman, Oklahoma 73019

Professor R. Neilson
Department of Chemistry
Texas Christian University
Fort Worth, Texas 76129

Professor M. Newcomb
Department of Chemistry
Texas A&M University
College Station, Texas 77843

Professor L. Miller
Department of Chemistry
University of Minnesota
Minneapolis, Minnesota 55455

Professor K. O. Christe
Rockwell International
Canoga Park, California 91304

END

3-87

DTIC